Available online at www.sciencedirect.com
ScienceDirect
International Journal of Thermal Sciences 48 (2009) 618–625
International Journal of Thermal Sciences
www.elsevier.com/locate/ijts

Effects of a baffle on separated convection flow adjacent to backward-facing step

J.H. Nie *, Y.T. Chen, H.T. Hsieh

Department of Mechanical Engineering, University of Nevada, Las Vegas, 4505 Maryland Parkway, Las Vegas, NV 89154, USA

Received 26 November 2007; received in revised form 21 May 2008; accepted 21 May 2008

Available online 20 June 2008

Abstract

Numerical simulations of three-dimensional laminar forced convection flow adjacent to backward-facing step in rectangular duct are presented to examine effects of the baffle on flow and heat transfer distributions. The step height is maintained as constant. A baffle is mounted onto the upper wall and its distance from the backward-facing step is varied. The inlet flow is hydrodynamically steady and fully developed with uniform temperature. The Reynolds number based on the double height of the duct upstream of the step is equal to 343. The bottom wall is heated with constant heat flux, while other walls are maintained as being thermally adiabatic. Velocity, temperature, Nusselt number, and friction coefficient distributions are presented. A baffle mounted onto the upper wall increases the magnitude of maximum Nusselt number at the stepped wall. One segment of the x_u-line developing close to the backward-facing step becomes shorter with decrease of the distance of the baffle from the backward-facing step. It becomes more relatively uniform in the spanwise direction as the distance of the baffle from the backward-facing step decreases. The other segment developing adjacent to the sidewall moves further downstream as the baffle moves in the streamwise direction away from the backward-facing step. The maximum Nusselt number on the stepped wall develops near the sidewall, and it moves further downstream as the location of the baffle moves in the streamwise direction. The friction coefficient at the stepped wall decreases as the distance of the baffle from the inlet increases.

Keywords: Backward-facing step; Heat transfer enhancement; Numerical simulations; Baffle

1. Introduction

Convection flow and heat transfer in channels with abrupt expansion in flow geometry are widely encountered in engineering applications and thermal systems, such as cooling passages of turbine blades, diffusers, combustors, and heat exchangers. In the flow reattachment region a great deal of mixing of high and low energy fluid occurs, thus significantly impacting the flow and heat transfer performance of these devices. In particular, momentum and thermal transports in the reattaching flow region and inside the reverse flow regions vary greatly. For example, the minimum wall shear stress and the maximum heat transfer rate occur in the neighborhood of reattaching flow region, while the minimum heat transfer rate occurs at the corner where the sudden change in flow geometry starts. Studies on separated-reattached convection flow have been extensively conducted during the past decades, and the backward-facing step geometry received most of the attention (see, for example, [1,2] and the references cited therein). This geometry is simple, yet the flow and the heat transfer through it contain most of the features encountered in more complex geometries. In addition, the backward-facing step flow has been used in benchmark studies to validate simulation codes and algorithms [3,4].

Simulations and measurements of flow adjacent to the two-dimensional (2-D) backward-facing step geometry have extensively appeared in the literature [5,6]. These results indicated that the flow separation and subsequent recirculation result in very poor heat transfer performance in the region near the backward-facing step. The compactness of new thermal systems drives the importance of finding effective means for facilitating heat transfer. Study of the backward-facing step with various baffles is one method to accomplish this on a simple

* Corresponding author.
E-mail address: jianhu@nscee.edu (J.H. Nie).

1290-0729/$ – see front matter
doi:10.1016/j.ijthermalsci.2008.05.015

Nomenclature

AR	aspect ratio $= W/S$
C_f	skin friction coefficient $= 2\tau_w/\rho u_0^2$
C_p	specific heat
D	normalized distance of the baffle from the sudden expansion $= d/H$
d	distance of the baffle from the sudden expansion
ER	expansion ratio $= H/(H-S)$
H	duct height downstream of the step
h	duct height upstream of the step
h_b	baffle height
k	thermal conductivity
L	half width of the duct
Nu	Nusselt number $= q_w S/k(T_w - T_0)$
p	pressure
q_w	wall heat flux $= -k\partial T/\partial y\|_{\text{at the wall}}$
Re	Reynolds number $= 2\rho u_0 h/\mu$
S	step height
T	temperature
T_0	inlet temperature
T_w	wall temperature
u	velocity component in the x-coordinate direction
u_0	average inlet velocity
v	velocity component in the y-coordinate direction
W	width of the duct ($W = 2L$)
w_b	width of the baffle
w	velocity component in the z-coordinate direction
x	streamwise coordinate direction
x_u	locations where the streamwise velocity gradient is zero ($\partial u/\partial y = 0$)
x_w	locations where the spanwise velocity gradient is zero ($\partial w/\partial y = 0$)
y	transverse coordinate direction
z	spanwise coordinate direction

Greek symbols

μ	dynamic viscosity
ρ	density
τ_w	wall shear stress $= \mu\sqrt{(\partial u/\partial y)^2 + (\partial w/\partial y)^2}$

system which has much in common with many more complex heat exchanger systems.

Most of the industrial applications exhibit three-dimensional (3-D) behavior but most of the published studies are restricted to the two-dimensional case. Simulations of 3-D separated-reattached flow adjacent to backward-facing step by Chiang and Sheu [7,8], by Iwai et al. [9], by Carrington and Pepper [10], and very recently by Kitoh et al. [11] revealed some of the complex flow behaviors that develop in this geometry. Armaly et al. [12] showed the swirling spanwise flow inside the primary reverse flow region. The developments of a downwash adjacent to the sidewall and a swirling "jet-like" flow that impinges on the stepped wall near the sidewall in this geometry were illustrated by Nie and Armaly [13]. Effects of different parameters, such as aspect ratio [9], step height [14], and Reynolds number [15], on three-dimensional separated-reattached convection flow adjacent to backward-facing step are reported. All of these numerical and/or experimental studies brought to light the complex characteristics of flow and heat transfer in this geometry.

Little work has been published for dealing with how to alter the flow structure and temperature distribution, and then to attain the high heat transfer performance of three-dimensional separated convection flow adjacent to backward-facing step in channels. The use of porous inserts for heat transfer enhancement in recirculating flows over a backward-facing step was investigated by Martin et al. [16]. Recently, numerical simulations by Tsay et al. [17] revealed that the average Nusselt number can be enhanced by placing a baffle in the two-dimensional backward-facing step flow. To the best of the authors' knowledge, study of three-dimensional fluid flow and heat transfer adjacent to backward-facing step with a baffle has not been seen in the published literature. This fact, along with the realization that such geometry appears regularly in many industrial heat transfer devices, such as the heat exchanger, electronic cooling, and others, motivated the present study. The main objective of this study is to examine the heat transfer enhancement of separated convection flow adjacent to backward-facing step by using a baffle installation onto the channel wall.

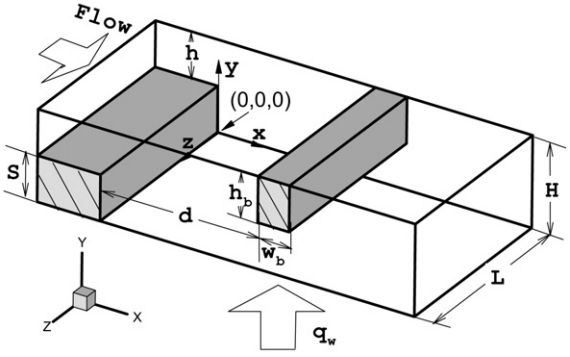

Fig. 1. Schematic of the computational domain.

2. Model description and numerical simulation

Three-dimensional laminar forced convection flow adjacent to backward-facing step in a heated rectangular duct with a baffle mounted on the upper wall is numerically simulated, and the computational domain is schematically shown in Fig. 1. The upstream height of the duct (h) is 0.01 m, its downstream height (H) is 0.02 m, and its width (W) is 0.08 m. This geometry provides a backward-facing step height (S) of 0.01 m, an expansion ratio of $ER = H/(H-S) = 2$, and an aspect ratio of $AR = W/S = 8$. The selection of the values for these parameters is motivated by the fact that laser-Doppler measurements [18] are available for this geometry and they can

be used to validate the flow simulation code. A baffle is installed on the upper wall of the backward-facing step geometry and its relative position is shown in Fig. 1. Both the baffle's width (w_b) and height (h_b) are kept as 0.01 m. The distance of the baffle from the backward-facing step is varied ($d = 0.02$, 0.05 and 0.08 m, respectively), for the purpose of examining the baffle effects. This provides the normalized distance ($D = d/H$) of 1, 2.5 and 4, respectively. The case of $D = \infty$ represents the backward-facing step flow without baffle. The length of the computational domain is 0.02 m and 0.5 m upstream and downstream of the sudden expansion respectively, i.e., $-2 \leqslant x/S \leqslant 50$. This choice is made to ensure that the flow at the inlet section of the duct ($x/S = -2$) is not affected significantly by the sudden expansion in the geometry at the step, and the flow at the exit section ($x/S = 50$) is fully developed. It was confirmed that the use of a longer computational domain did not change the flow behavior in the region close to the backward-facing step. Velocity measurements in the same geometry without the baffle show that the flow is laminar and steady for Reynolds number (Re) smaller than 500 [18]. By exploiting the symmetry of the flow field in the spanwise direction, the width of the computational domain is reduced to half of the actual width of the duct ($L = W/2 = 0.04$ m). The steady laminar three-dimensional Navier–Stokes and energy equations are solved numerically (using finite volume scheme) together with the continuity equation to simulate the thermal and the flow fields.

Continuity equation:

$$\frac{\partial}{\partial x}(\rho u) + \frac{\partial}{\partial y}(\rho v) + \frac{\partial}{\partial z}(\rho w) = 0 \tag{1}$$

Momentum equations:

$$\frac{\partial}{\partial x}(\rho uu) + \frac{\partial}{\partial y}(\rho uv) + \frac{\partial}{\partial z}(\rho uw) = -\frac{\partial p}{\partial x} + \mu\left(\frac{\partial^2 u}{\partial x^2} + \frac{\partial^2 u}{\partial y^2} + \frac{\partial^2 u}{\partial z^2}\right) \tag{2}$$

$$\frac{\partial}{\partial x}(\rho uv) + \frac{\partial}{\partial y}(\rho vv) + \frac{\partial}{\partial z}(\rho vw) = -\frac{\partial p}{\partial y} + \mu\left(\frac{\partial^2 v}{\partial x^2} + \frac{\partial^2 v}{\partial y^2} + \frac{\partial^2 v}{\partial z^2}\right) \tag{3}$$

$$\frac{\partial}{\partial x}(\rho uw) + \frac{\partial}{\partial y}(\rho vw) + \frac{\partial}{\partial z}(\rho ww) = -\frac{\partial p}{\partial z} + \mu\left(\frac{\partial^2 w}{\partial x^2} + \frac{\partial^2 w}{\partial y^2} + \frac{\partial^2 w}{\partial z^2}\right) \tag{4}$$

Energy equation:

$$\frac{\partial}{\partial x}(\rho C_p uT) + \frac{\partial}{\partial y}(\rho C_p vT) + \frac{\partial}{\partial z}(\rho C_p wT) = k\left(\frac{\partial^2 T}{\partial x^2} + \frac{\partial^2 T}{\partial y^2} + \frac{\partial^2 T}{\partial z^2}\right) \tag{5}$$

where T is temperature, p is pressure, and u, v, w are velocity components in coordinate directions of x, y, and z, respectively, as shown in Fig. 1 in this geometry. The physical properties are treated as constants in the simulation and evaluated for air at the inlet temperature of $T_0 = 20\,^\circ$C (i.e., density (ρ) equals to 1.205 kg/m^3, dynamic viscosity (μ) is 1.81×10^{-5} kg/m s, thermal conductivity (k) is 0.0259 W/m °C, and specific heat (C_p) is 1005 J/kg °C). The channel is placed horizontally and the buoyancy force can be neglected. The boundary conditions are treated as non-slip conditions at the solid walls (zero velocities), and thermally adiabatic at all the walls with the exception of the downstream stepped wall ($y/S = 0.0$, for $0 \leqslant x/S \leqslant 50$ and all z) that was treated as having a fixed and uniform heat flux ($q_w = -k\partial T/\partial y|_{y=0}$) that is equal to 50 W/m^2. The flow rate was maintained as being constant with a Reynolds number ($Re = 2\rho u_0 h/\mu$) of 343, because for this Reynolds number there is experimental data available for the backward-facing step flow without the baffle [18]. The flow conditions at the upstream inlet section of the duct ($x/S = -2$, $1 \leqslant y/S \leqslant 2$, for all z) are considered to be hydrodynamically steady and fully developed, and having a uniform temperature profile ($T_0 = 20\,^\circ$C). Distribution of the mean streamwise velocity component (u) is considered to be equivalent to the one described by Shah and London [19], while the other velocity components (v and w) are set equal to zero at that inlet section ($x/S = -2$). Symmetry conditions were imposed at the center width of the duct ($z/L = 1$, for all x and y), and fully developed flow and thermal conditions were imposed at the exit section of the computational domain ($x/S = 50$, for all y and z).

Numerical solution of the governing equations together with the boundary conditions was performed by utilizing SIMPLE algorithm [20] for the pressure correction in the iteration procedure. Hexahedron volume elements and non-uniform staggered grid arrangement are employed in the simulation. The grid is highly concentrated close to the step, near the corners and adjacent to the solid wall boundaries, in order to ensure the accuracy of the numerical simulation. This flow simulation code was developed in the FORTRAN programming language. It was used in previous studies [13,14], and its description and validation can be found in these references. Results from several grid densities for the case without baffle ($D = \infty$) were used in developing a grid independent solution for this study. The velocity and temperature values at a selected point ($x/S = 10$, $y/S = 1$ and $z/L = 0.5$) within the flow domain and the x_u-line which designates the locations where the mean streamwise velocity component (u) is zero adjacent to the stepped wall are presented in Table 1 for different computational grids. A grid of $180 \times 50 \times 36$ downstream from the step was selected for these simulations. Using a finer grid of $250 \times 60 \times 42$ resulted in less than 1% difference in the predicted results. The convergence criterion required that the maximum relative mass residual based on the inlet mass be smaller than 10^{-6}. Predictions of the locations where the mean streamwise velocity component (u) is zero on a plane adjacent to the stepped wall (line (x_u)) compare very well with laser-Doppler measured results [18] for $D = \infty$, as shown in Fig. 2, and that provides code validation.

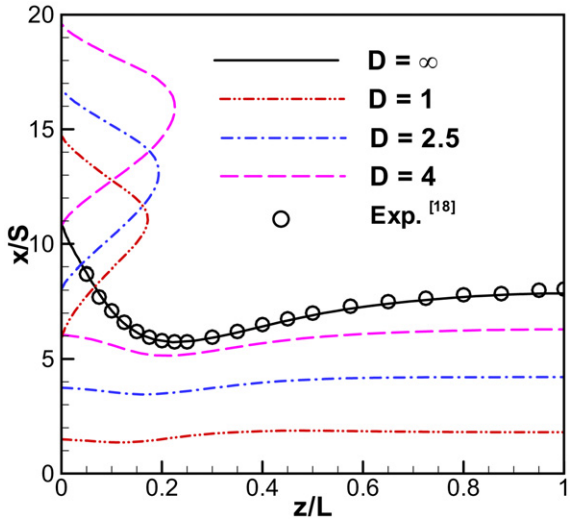

Fig. 2. Distributions of the x_u-lines on the stepped wall.

3. Results and discussions

3.1. Effects of a baffle on the x_u-lines

Distributions of the x_u-lines adjacent to the stepped wall are shown in Fig. 2 for different streamwise locations of the baffle. This line is a link of locations along the spanwise direction where the streamwise velocity component (u) is zero or changes its sign adjacent to the stepped wall. It is usually used as the reattachment location for 2-D flow in this geometry or at the center of the three-dimensional duct with very large aspect ratio [12,14]. In 3-D case, the maximum length in its spanwise distribution appears at the sidewall ($z/L = 0$) and the minimum develops near the sidewall ($z/L \approx 0.25$) for $D = \infty$. This is the result of the "jet-like" flow impingement onto the stepped wall and the recirculation region adjacent to the sidewall, as noted by Nie and Armaly [12]. For the standard backward-facing step flow (without baffle), there is only one x_u-line on the stepped wall. However, for the backward-facing step flow with a baffle on the upper wall, the x_u-line consists of two segments as the baffle moves toward the backward-facing step. One of the segments develops near the backward-facing step and it becomes shorter with the decrease of the normalized distance, D. It becomes relatively uniform in the spanwise direction, and the rapid change in its spanwise distribution near the sidewall cannot be seen clearly. The other segment developing adjacent to the sidewall moves further downstream with the increase of D as the baffle moves along the streamwise direction. Its size in the spanwise direction also becomes greater as the distance increases.

Distributions of the x_u-lines adjacent to the sidewall are presented in Fig. 3. Although this line is not identical to the outer edge of the recirculation region for three-dimensional backward-facing step flow, it can still be used to identify the approximate size of the recirculation regions near the sidewall. The primary recirculation region which develops adjacent to the backward-facing step and the stepped wall becomes larger in the streamwise direction as the baffle moves further downstream in the streamwise direction. The recirculation region behind the baffle and adjacent to the upper wall also moves further downstream with the increase of D from 1 to 4. The recirculation region upstream of the baffle and adjacent to the upper wall becomes larger in length in the x-direction as the distance of D increases. Another recirculation region which develops adjacent to the stepped wall ($y/S = 0$) and downstream of the primary recirculation region moves further downstream with the increase of D. But, this recirculation region is not observed any more for the case without baffle ($D = \infty$).

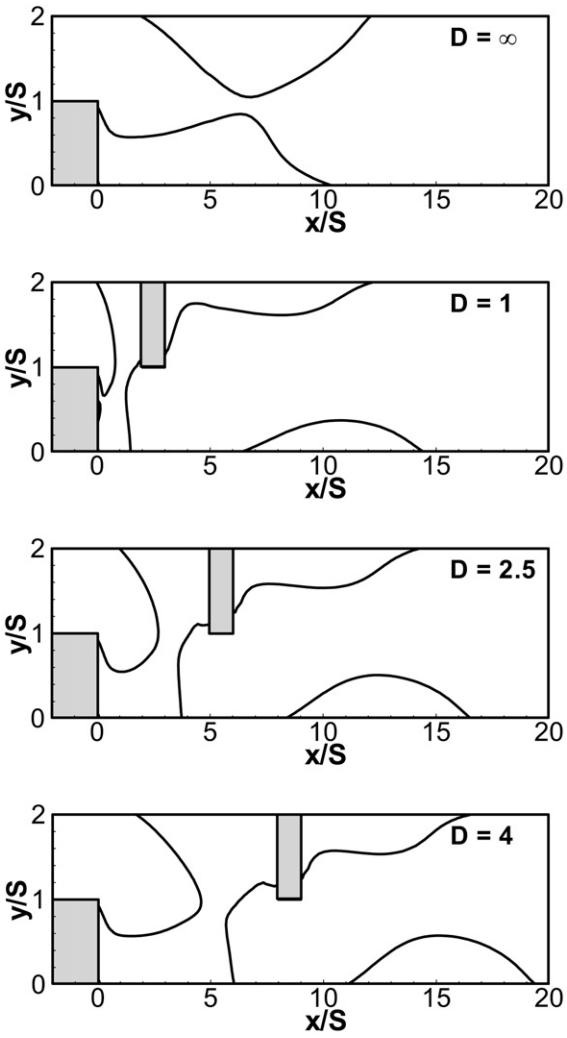

Fig. 3. Distribution of the x_u-lines adjacent to the sidewall ($z/L = 0.01$).

3.2. Effects of the baffle on the general flow features

The general flow features can be seen more clearly from the limiting streamlines [21] adjacent to the stepped wall ($y/S = 0$), the sidewall ($z/L = 0$) and the upper wall ($y/S = 2$), as exhibited in Fig. 4. The baffle is also included in the figure (wherever it is installed) in order to show its relative location. One recirculation region appears near the sidewall for the backward-facing step flow without baffle ($D = \infty$) as shown in Fig. 4(a). As a result of the mounted baffle onto the upper wall, this recirculation region is separated into two regions in front of and

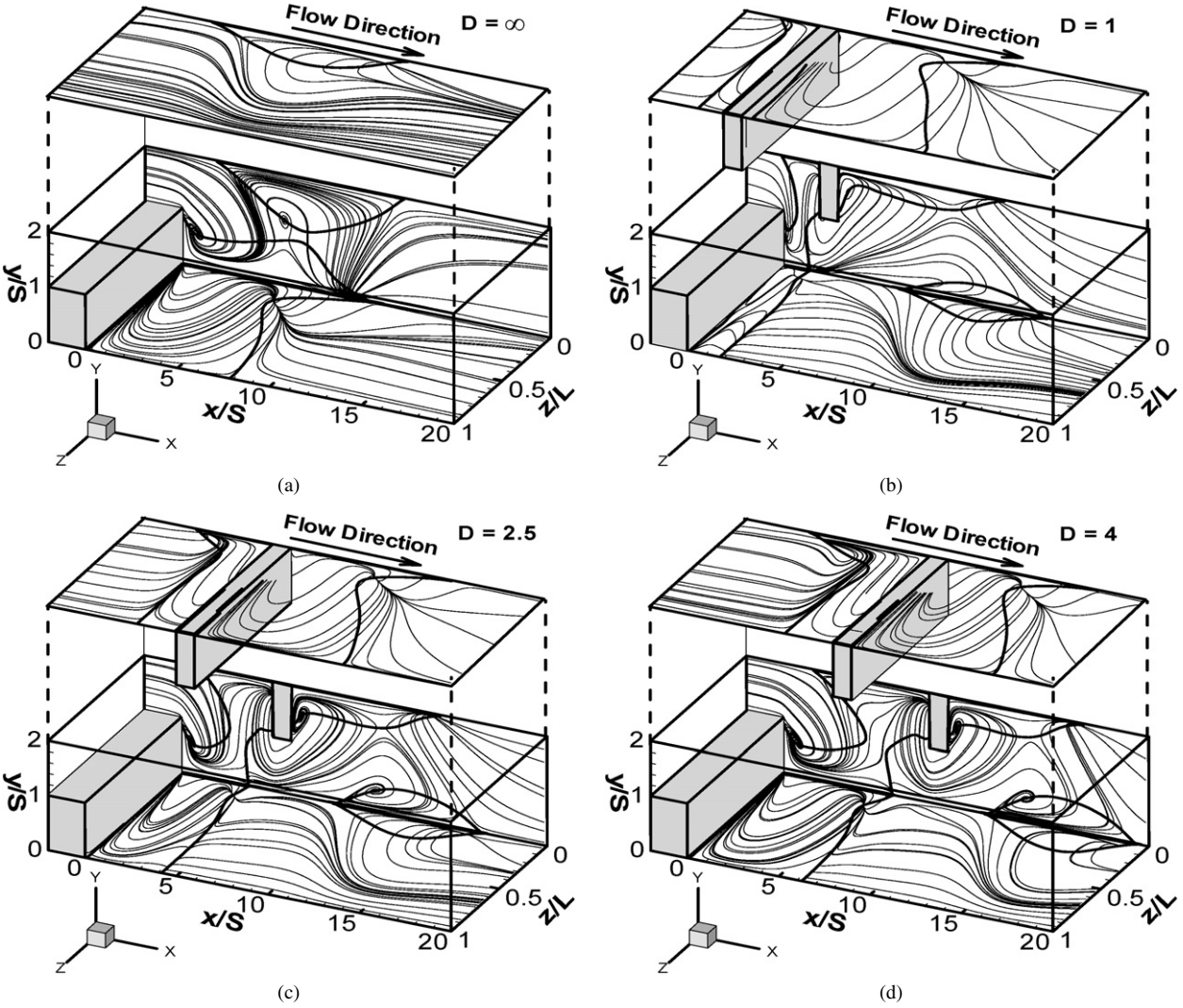

Fig. 4. Limiting streamlines adjacent to the bounding walls.

behind the baffle. The "jet-like" flow impinges onto the stepped wall, as identified as a singular point, i.e., the "source" location of the limiting streamlines in the figure. The primary recirculation region adjacent to the backward-facing step and the stepped wall becomes greater as the location of the baffle moves further downstream. Another recirculation region develops adjacent to the stepped wall and the bottom of the sidewall as the baffle is mounted onto the upper wall.

3.3. Effects of the baffle on heat transfer

Distributions of the Nusselt number at the heated stepped wall are presented in Fig. 5. Because of the applied boundary condition of constant heat flux, the maximum Nusselt number is inversely proportional to the minimum wall temperature. The location of the maximum Nusselt number is also included in the figure. The maximum Nusselt number develops near the sidewall, and it moves further downstream as the location of the baffle moves along the streamwise direction. The "jet-like" flow impingement location is also included in the figure. It appears near the location of the maximum Nusselt number, but closer to the backward-facing step. The magnitude of the maximum Nusselt number increases as the baffle moves toward the backward-facing step (with the decrease of D). This can also be seen from the Nusselt number distributions along the center of the duct, as shown in Fig. 6. For instance, the maximum Nusselt number for $D = 1$ is about three times of the one for $D = \infty$ (without baffle). They become close to each other and asymptotically approach the value for the fully developed duct flow as $x/S > 20$.

Distributions of the temperature fields at the sidewall ($z/L = 0$) are shown in Fig. 7. The maximum temperature develops near the corner of the backward-facing step and the stepped wall, where the heat exchanging rate is poor. As the baffle distance (D) increases, the maximum temperature becomes higher. Fig. 8 shows the friction coefficient distributions on the stepped wall. The friction coefficient at this wall decreases as the baffle distance (D) increases. This can also be observed from the distribution of the friction coefficient at the stepped wall along the center width of the duct, as exhibited in Fig. 9. They asymptotically approach the value for the fully developed duct flow as $x/S > 20$.

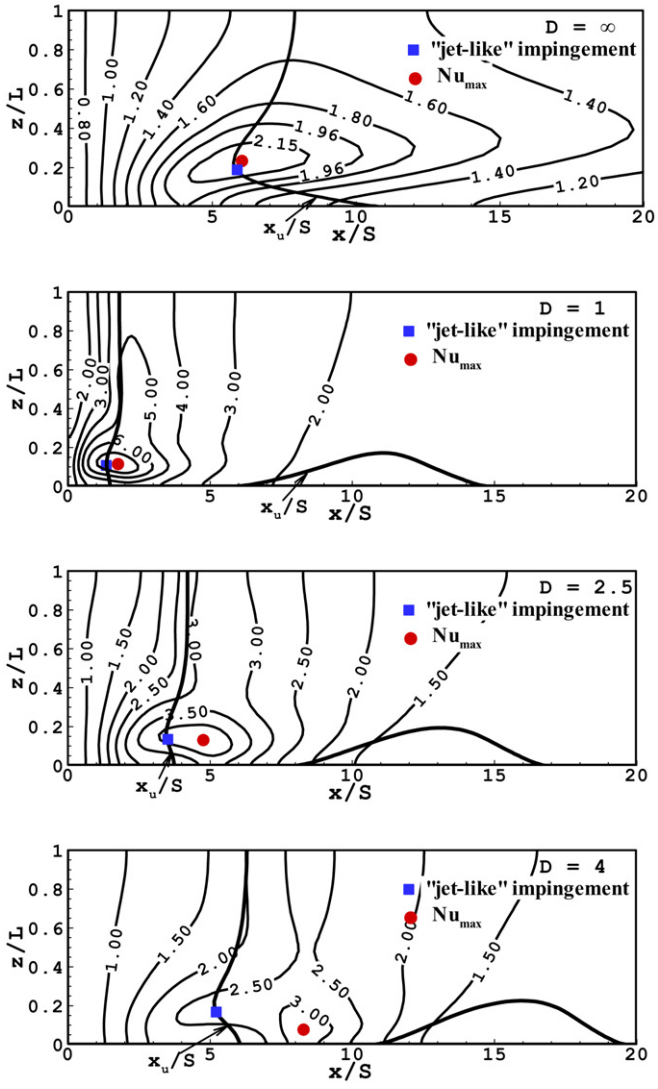

Fig. 5. Nusselt number distribution on the heated stepped wall.

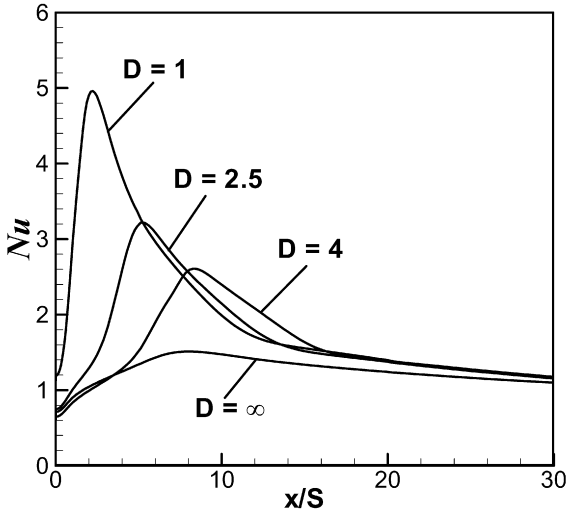

Fig. 6. Nusselt number distributions on the stepped wall along the center of the duct.

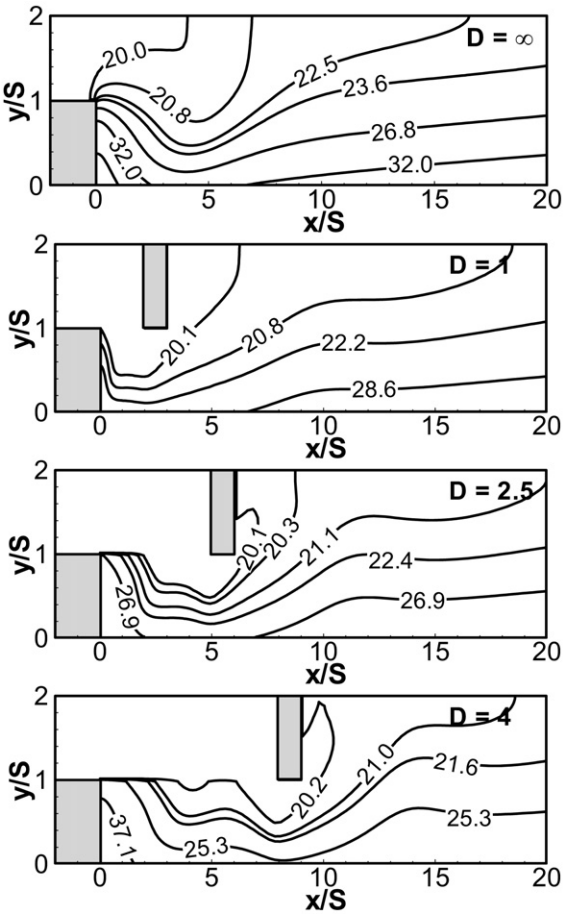

Fig. 7. Temperature distributions on the sidewall.

Table 1
Velocities and temperatures at $x/S = 10$, $y/S = 1$, and $z/L = 0.5$ and the x_u-line locations for different computational grids

Grid	Size ($x \times y \times z$)	u (m/s)	T (°C)	x_u/S at $z/L = 1$
1	50×15 × 15	0.265436	20.9122	8.330
2	50×28 × 20	0.268848	20.7985	8.153
3	80×28 × 20	0.271604	20.7878	7.632
4	120×28 × 20	0.273762	20.7832	7.735
5	150×30 × 25	0.276255	20.7610	7.801
6	180×40 × 30	0.278677	20.7474	7.858
7	200×50 × 36	0.279824	20.7328	7.884
8	250×60 × 42	0.280198	20.7302	7.893

Velocity fields adjacent to the stepped wall are shown in Fig. 10 for the cases of $D = 2.5$ and ∞. Different colors represent different magnitudes of the normal velocity component to this wall, which is the v-velocity component in the present simulations. The x_u-line along which the u-velocity component is zero and the x_w-line where the w-velocity component is zero are also included in this figure. The circle symbol denotes the "jet-like" flow impingement location where both the u- and the w-velocity components are equal to zero. For the backward-facing step flow without baffle, only one "jet-like" impingement location is observed. Another one which develops adjacent to the sidewall can be seen for $D = 2.5$. Fig. 10

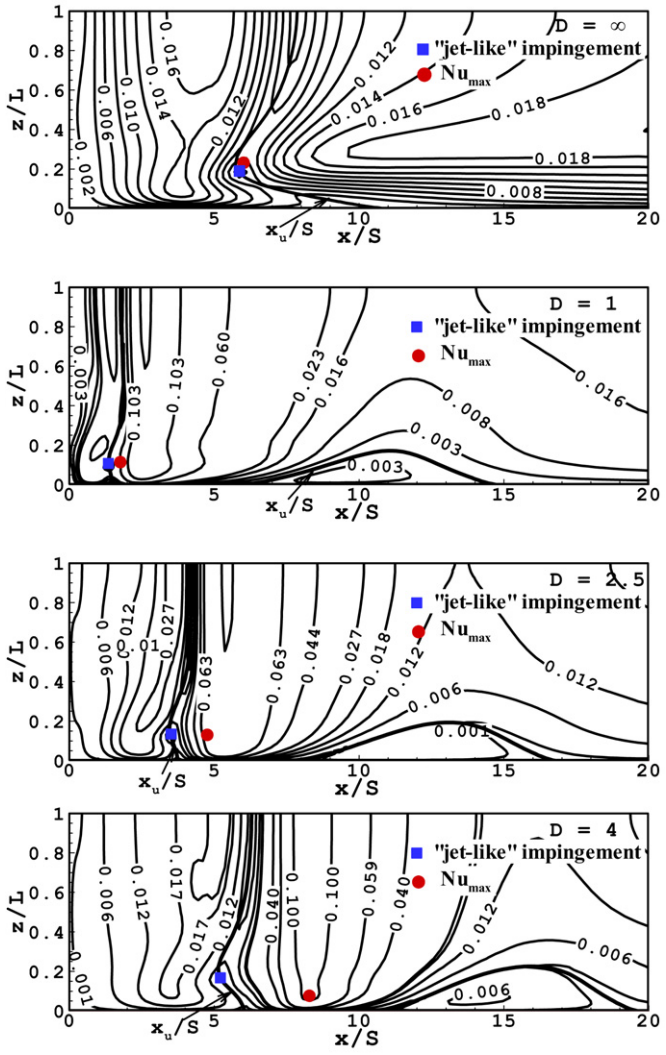

Fig. 8. Friction coefficient distribution on the stepped wall.

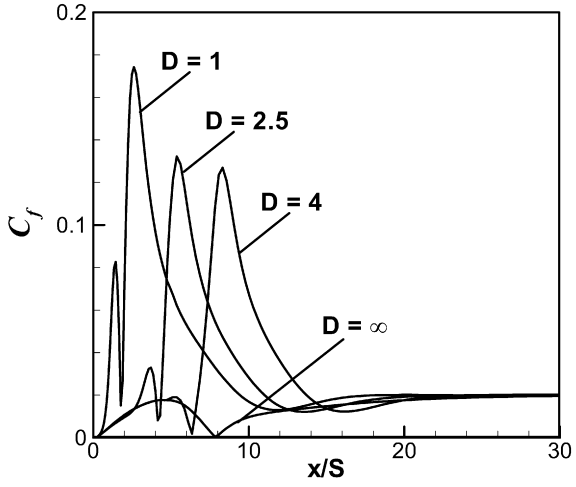

Fig. 9. Friction coefficient distribution along the center of the duct.

also shows that the magnitude of the v-velocity component (the absolute value) is increased with the installation of a baffle on the upper wall.

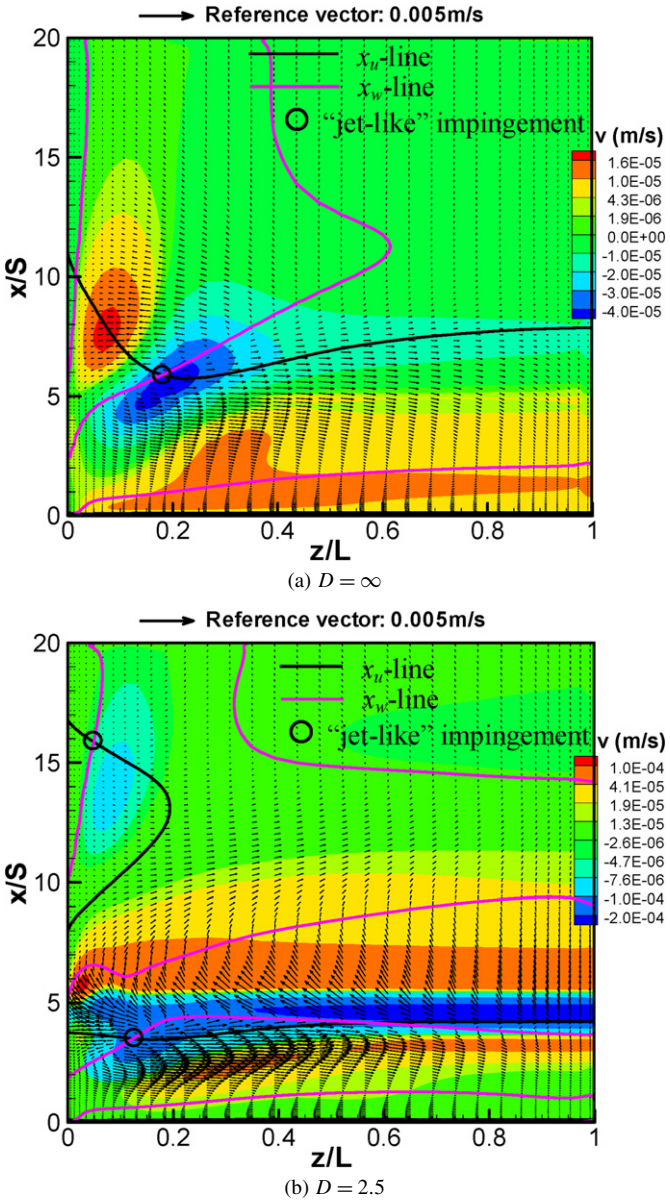

Fig. 10. Velocity fields adjacent to the stepped wall.

4. Conclusions

Results from numerical simulations of three-dimensional laminar forced convection flow adjacent to backward-facing step in a rectangular duct are used to examine effects of a baffle on the flow and heat transfer in this geometry. The Reynolds number based on the double height of the duct upstream of the step is equal to 343. Installation of a baffle onto the upper wall enhances heat transfer and increases the magnitude of maximum Nusselt number at the stepped wall. One segment of the x_u-line develops close to the backward-facing step and it becomes shorter as the distance of the baffle from the backward-facing step decreases. It becomes more relatively uniform in the spanwise direction, and the rapid change in its spanwise distribution near the sidewall cannot be clearly seen as the distance decreases. The other segment of x_u-line developing adjacent to the sidewall moves further downstream as the baffle moves in

the streamwise direction. The maximum Nusselt number develops near the sidewall, and it moves further downstream as the location of the baffle moves in the streamwise direction. The friction coefficient at the stepped wall decreases as the distance of the baffle from the inlet increases. The magnitude of the normal velocity component adjacent to the stepped wall (the absolute value) is increased with the installation of a baffle on the upper wall.

Acknowledgements

This work was supported in part by US Department of Energy under award DE-FG36-03GO13063, NASA EPSCoR Award, and Department of Defense (Army Research Laboratory) under award DAAD19-03-2-0007.

References

[1] R.L. Simpson, Aspects of turbulent boundary-layer separation, Progress in Aerospace Sciences 32 (5) (1996) 457–521.
[2] J.K. Eaton, J.P. Johnson, A review of research on subsonic turbulent flow reattachment, AIAA Journal 19 (9) (1981) 1093–1100.
[3] B.F. Blackwell, B.F. Armaly (Eds.), Computational Aspects of Heat Transfer – Benchmark Problems, HTD, vol. 258, American Society of Mechanical Engineers, New York, NY, 1993, pp. 1–115.
[4] J.L. Sohn, Evaluation of FIDAP on some classical laminar and turbulent benchmarks, International Journal for Numerical Methods in Fluids 8 (12) (1988) 1469–1490.
[5] B.F. Armaly, F. Durst, J.C.F. Pereira, B. Schonung, Experimental and theoretical investigation of backward-facing step flow, Journal of Fluid Mechanics 127 (12) (1983) 473–496.
[6] P.R. Kanna, M.K. Das, Conjugated heat transfer study of a two-dimensional laminar incompressible wall jet over a backward-facing step, ASME Journal of Heat Transfer 129 (2) (2007) 220–231.
[7] T.P. Chiang, T.W.H. Sheu, Vortical flow over a 3-D backward-facing step, Numerical Heat Transfer Part A – Applications 31 (2) (1997) 167–192.
[8] T.P. Chiang, T.W.H. Sheu, A numerical revisit of backward-facing step flow problem, Physics of Fluids 11 (4) (1999) 862–874.
[9] H. Iwai, K. Nakabe, K. Suzuki, Flow and heat transfer characteristics of backward-facing step laminar flow in a rectangular duct, International Journal of Heat and Mass Transfer 43 (3) (2000) 457–471.
[10] D.B. Carrington, D.W. Pepper, Convective heat transfer downstream of a 3-D backward-facing step, Numerical Heat Transfer Part A – Applications 41 (6–7) (2002) 555–578.
[11] A. Kitoh, K. Sugawara, H. Yoshikawa, T. Ota, Expansion ratio effects on three-dimensional separated flow and heat transfer around backward-facing steps, ASME Journal of Heat Transfer 129 (9) (2007) 1141–1155.
[12] B.F. Armaly, A. Li, J.H. Nie, Three-dimensional forced convection flow adjacent to backward-facing step, AIAA Journal of Thermophysics and Heat Transfer 16 (2) (2002) 222–227.
[13] J.H. Nie, B.F. Armaly, Reattachment of three-dimensional flow adjacent to backward-facing step, ASME Journal of Heat Transfer 125 (3) (2003) 422–428.
[14] J.H. Nie, B.F. Armaly, Three-dimensional convective flow adjacent to backward-facing step – effects of step height, International Journal of Heat and Mass Transfer 45 (12) (2002) 2431–2438.
[15] J.H. Nie, B.F. Armaly, Reverse flow regions in three-dimensional backward-facing step flow, International Journal of Heat and Mass Transfer 47 (22) (2004) 4713–4720.
[16] A.R. Martin, C. Saltiel, W. Shyy, Heat transfer enhancement with porous inserts in recirculating flows, ASME Journal of Fluids Engineering 120 (2) (1998) 458–467.
[17] Y.L. Tsay, T.S. Chang, J.C. Cheng, Heat transfer enhancement of backward-facing step flow in a channel by using baffle installation on the channel wall, Acta Mechanica 174 (1–2) (2005) 63–76.
[18] B.F. Armaly, A. Li, J.H. Nie, Measurements in three-dimensional separated flow, International Journal of Heat and Mass Transfer 46 (19) (2003) 3573–3582.
[19] R.K. Shah, A.L. London, Laminar Forced Convection in Ducts, Academic Press, New York, NY, 1978.
[20] S.V. Patankar, Numerical Heat Transfer and Fluid Flow, Hemisphere, New York, NY, 1980.
[21] A.E. Perry, M.S. Chong, Interpretation of flow visualization, in: A.J. Smits, T.T. Lim (Eds.), Flow Visualization: Techniques and Examples, Imperial College Press, London, UK, 2000, pp. 1–26.